Upwelling features off the coast of north-western Africa in 2009-2013

M. Menna[1], S. Faye[2,5], P.-M. Poulain[1], L. Centurioni[3], A. Lazar[4,5], A. Gaye[5], B. Sow[6,5] and D. Dagorne[7]

[1] *Istituto di Oceanografia e Geofisica Sperimentale - OGS, Sgonico (TS), Italy*

[2] *Centre de Recherches Océanographiques Dakar-Thiaroye (CRODT), Dakar, Sénégal*

[3] *Scripps Institution of Oceanography, UCSD, La Jolla, California*

[4] *CNRS/IRD, Paris, France*

[5] *LPAOF/UCAD, Dakar, Senegal*

[6] *Université de Ziguinchor, Sénégal*

[7] *Institute de Recherche pour le Développement, Plouzané, France*

ABSTRACT Satellite data (images of sea surface temperature and chlorophyll-a), ocean surface wind products, Lagrangian observations (surface drifters) and other ancillary data (upwelling index) are used to describe the upwelling seasons off NW Africa during 2009-2013, with particular focus on the coasts of Senegal and Mauritania. The impact of the upwelling is characterised by a comparative analysis, carried out in terms of wind-induced upwelling and water/ecosystem response to this forcing, of five geographical sectors detected in the study area. The wind forcing analysis shows the most favourable upwelling conditions in the period December-June in the southern sectors (south of 16° N), and from February to October in the northern sectors (north of 18° N). Southern sectors are strongly influenced by wind forcing, whereas to the north the upwelling also occurs during the months with low Ekman transport values. The analysis of the sea surface temperature and chlorophyll-a concentration confirms the existence of an upwelling season during winter-spring in the south, and emphasizes the different behaviours between the northern and southern sectors. Drifter tracks allow the addition of details about the flow of cold water offshore and alongshore. In particular, they describe the westward transport of cold water, by means of energetic filaments rooted at specific locations along the coast, north of Cape Vert and the south-SW ward transport of the coastal water south of Cape Vert.

1. Introduction

The Canary Current Upwelling System (CCUS), which extends from the Iberian Peninsula (43° N) to the south of Senegal (8° N), is one of the four major eastern boundary upwelling regions of the world oceans (Santos *et al.*, 2005; Aristegui *et al.*, 2009; Benazzouz, 2014) and sustains large fisheries resources (Marchesiello *et al.*, 2004). Upwelling events in this region are triggered by the northeasterly alongshore trade winds, which drive the surface Ekman transport offshore. The strength of the winds is modulated by the seasonal migration of the Intertropical Convergence Zone and of the Azores high-pressure cell (Wooster *et al.*, 1976; Mittelstaedt,
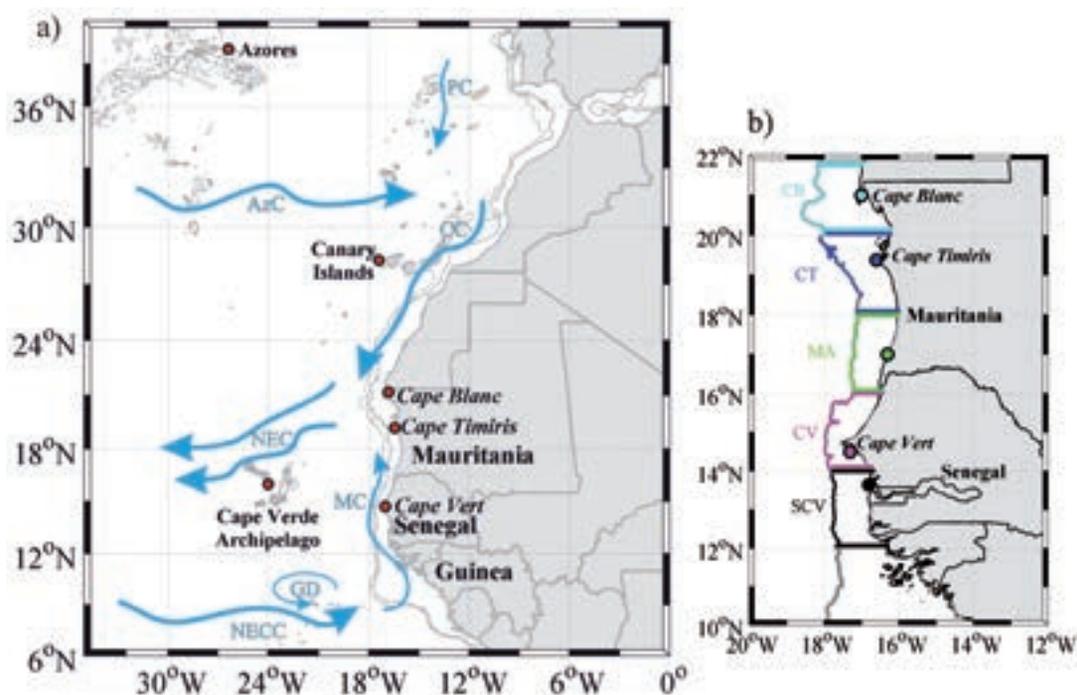
Fig. 1 - a) Geography, bathymetry and main surface current systems off the coast of NW Africa in the region surrounding the Cape Vert Archipelago. The 1000 m and 2000 m isobaths are shown with light grey lines. b) Coastal area, enclosed between the coast and the 2000 m isobath, used to estimate the Hovmoller diagrams of Fig. 2; colours point out the sectors used to compute the time series of Figs. 3 and 4. The acronyms are explained in the text.

1991; Mason *et al.*, 2011). The meridional shift of the trade winds causes seasonal upwelling variability in the extreme north and south regions of the CCUS, while in the central region upwelling is relatively continuous year round (Wooster *et al.*, 1976; Aristegui *et al.*, 2004). The upwelled relatively cold and nutrient-rich coastal waters mostly flow offshore in filaments rooted at specific locations along the coast (Demarcq, 1998; Meunier *et al.*, 2012); eddies transport nutrients from the upwelling region westwards in the oligotrophic north Atlantic (Lumpkin and Garzoli, 2005; Alpers *et al.*, 2013).

The large-scale circulation in the CCUS (Fig. 1a) is dominated by the eastern branch of the North Atlantic subtropical gyre composed of the Azores (AzC), Portugal (PC), and Canary Currents (CC) (Barton, 1998; Lathuiliére, 2008). South of 20° N, the CC flows southwestwards and joins the North Equatorial Current (NEC) (Mittelstaedt, 1991), which forms the southern part of the subtropical gyre. Between 5° N and 10° N, the dominant feature is the eastward flow known as the North Equatorial Counter Current (NECC) (Lázaro *et al.*, 2005). Near the African coast, part of the NECC turns northwards, forming the Mauritania Current (MC). The MC shows a strong seasonal variability associated with the NECC and the wind field intensities. In winter and early spring, the NECC is weaker, the wind is favourable to coastal upwelling between 14° N and 20° N, and the MC is located south of 15 °N. In summer and early autumn, the strengthening of the NECC and the relaxation of the northeasterly trade winds favour the northward migration of the MC, which can reach as far as 20 °N (Lázaro *et al.*, 2005). SE of the Cape Vert Archipelago, there is a large-scale cyclonic circulation associated with the NEC, the NECC, and the MC, and called the Guinea Dome (GD). The core of this structure is located

near 9° N, 25° W in the summer months, at 10.5° N, 22° W in the winter months (Stramma *et al.*, 2005), and near 12° N, 26° W in fall (Doi *et al.*, 2009).

The southern portion of the CCUS, defined in this paper as the region between 12° N and 22° N (see Fig. 1 for geographical references), is characterised by upwelling events with a marked seasonal periodicity and with maximal intensity in winter (Wooster *et al.*, 1976; Aristegui *et al.*, 2004, Ndoye *et al.*, 2014). In the framework of the COCES (Coastal Ocean Circulation Experiment off Senegal) and COCES II projects, this region was deeply investigated with the aim of describing its peculiar upwelling features. The COCES and COCES II projects led to the deployment of more than 100 drifters off the Senegal coast in the period 2009-2013. The tracks of these drifters were used in concert with satellite data-sea surface temperature (SST) and chlorophyll-a concentration (Chl-a)-and other ancillary data (upwelling index and re-analysis wind) to improve our knowledge of the north-western Africa upwelling system with particular focus on the Senegal and Mauritania coastal areas. The study area was divided into five geographical sectors, and the different upwelling features of these sectors and the relative implications for the ecosystem as well as the main circulation features related with the transport of cold waters were analysed and compared. Details about the data used in this study are illustrated in Section 2, and a description of the intra- and inter-annual variability of the upwelling seasons 2009-2013 are presented in Section 3. Sections 4 and 5 include a discussion of the results and main conclusions.

2. Data and methods

1.1. Satellite data

Moderate Resolution Imaging Spectroradiometer (MODIS) 8-day composite maps of SST and Chl-a (http://oceancolor.gsfc.nasa.gov/DOCS/) focused on the region 8°-22° N, 12°-22° W and, gridded with a spatial resolution of ~5 km, were used to define the main characteristic of the upwelling season along the Senegal and Mauritania coasts in the period 2009-2013. The spatial (latitudinal) and temporal extensions of the upwelling events were identified using Hovmoller diagrams of the zonally averaged SST over the coastal area extending from the coast to the 2000 m isobath (Fig. 1b). This area was divided into five sectors according to the latitudinal evolution of the SST and the geographical characteristic of the region (see Fig. 16). More specifically, three sectors are located around the main capes and the other two in the region between the capes (South of Cape Vert-SCV; Cape Vert-CV; Southern Mauritania Coast-MA; Cape Timiris-CT; Cape Blanc-CB). Time series of the monthly spatially averaged SST obtained in each sector were used to describe the annual and inter-annual fluctuations related to upwelling processes. The surface cooling from the upwelled water reaching the sea surface is a potential proxy of the upwelling intensity (Benazzouz *et al.*, 2014).

The flow of cold water along the Senegal and Mauritania coasts was qualitatively described superimposing the COCES/COCES II drifter tracks on the normalised SST anomaly maps (see Subsection 2.4 for more details about drifter data). The normalised SST anomaly is obtained by subtracting the mean value of SST from the MODIS composite maps and dividing by the corresponding standard deviation. Representative snapshots of the main upwelling episodes were selected and are shown in Subsection 3.3.

2.2. Upwelling index

Ekman transport data provided by the NOAA Environmental Research Division (Upwelling and Environmental Index Products, http://www.pfeg.noaa.gov) were downloaded for the period 2009-2013. Ekman mass transport is defined as the wind stress divided by the Coriolis parameter; it is resolved into components parallel or normal to the local coastline orientation. Upwelling index from Ekman transport data (UI_E) can be calculated as the magnitude of the transport component in the direction perpendicular to the shoreline (Gomez-Gesteira *et al.*, 2008) and represents the volume per unit of time of the water being upwelled from the base of the Ekman layer. The monthly averaged coastal upwelling index UI_E was considered at five points along the coast (colored circles in Fig. 1b), each one located in a sector (SCV 13.8° N - 16.8° W; CV 14.5° N - 17.5° W; MA 17° N - 16° W; CT 19.4° N - 16.6° W; CB 21° N - 17° W). Generally, positive (negative) UI_E values mean upwelling favourable (unfavourable) conditions. In the southern CCUS, the monthly averaged UI_E shows a pronounced seasonality related to the upwelling and non-upwelling conditions, but it is positive everywhere (see Fig. 4a), creating the need to define a threshold to identify the upwelling events. The favourable upwelling conditions are established when $UI_E > 150$ m^3/s/100 m coastline, corresponding to meridional (upwelling favourable) wind intensities greater than 5 m/s in each sector of Fig. 1b.

2.3. Wind data

The time series of wind products were downloaded from the NOAA website (ERDDAP - NOAA/NCDC Blended Daily 0.25-degree Sea Surface Winds - Data Access Form). These products include globally gridded, high resolution ocean surface vector winds on a global 0.25° grid with a time resolution of 6 h. The wind speeds were generated by blending observations from multiple satellites; the wind directions came from two sources depending on the products: National Centers for Environmental Prediction (NCEP) reanalysis 2 or European Centre for Medium-range Weather (ECMWF).

2.4. Drifter data and processing

As part of the COCES and COCES II projects, 109 surface drifters were deployed off Senegal between May 2009 and June 2013. Two types of drifters were used: the Surface Velocity Program (SVP) drifter (Sybrandy and Niiler, 1991) and the Coastal Ocean Dynamic Experiment (CODE) drifter (Davis, 1985).

All drifters were tracked by polar-orbiting Argos satellites. The drifter position time series were edited of spikes and outliers, then linearly interpolated at regular 2-h intervals using the Kriging technique [optimal interpolation: Hansen and Poulain (1996), Poulain *et al.* (2004a)]. The interpolated positions were finally sub-sampled at 6-h intervals. Velocity components were then estimated from centered finite differences of 6-h subsampled positions. The entire data set includes 45232 6-h data points, corresponding to more than 30 drifter-years.

3. Results

Hovmoller diagrams of zonally averaged SST (Fig. 2) describe the main characteristics of the upwelling in the southern CCUS (area of averaging depicted in Fig. 1b) during the period 2009-
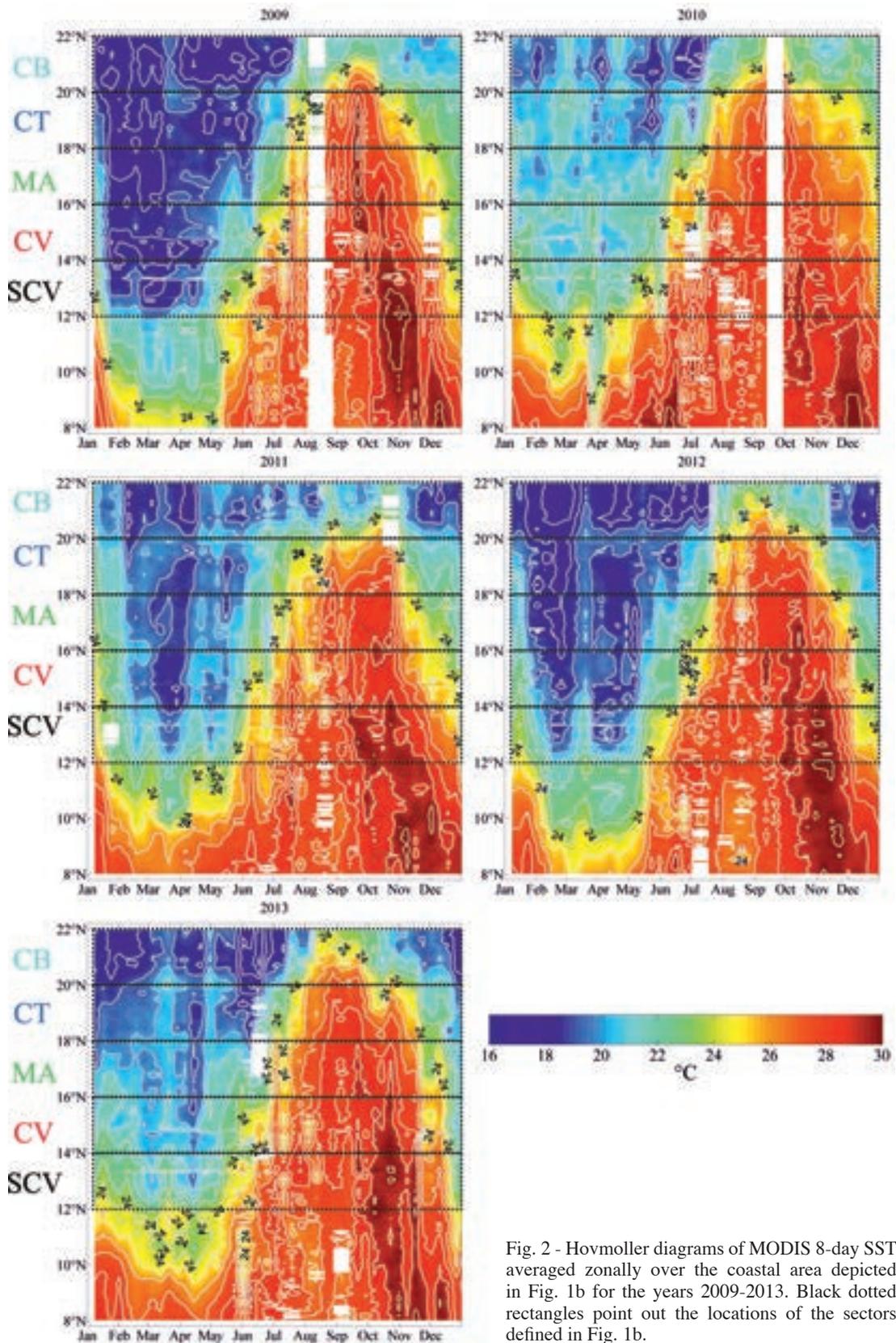
Fig. 2 - Hovmoller diagrams of MODIS 8-day SST averaged zonally over the coastal area depicted in Fig. 1b for the years 2009-2013. Black dotted rectangles point out the locations of the sectors defined in Fig. 1b.

2013. The isotherms of 24° C define the boundary between the cold upwelled and the warm resident waters. The area affected by upwelling is located north of 12° N and the length of the upwelling seasons increases with increasing latitude: they last from January to May in the SCV sector (12-14° N), from December/January to June in the CV sector (14-16° N), from December/January to June/July off the southern Mauritania coast (MA sector; 16° -18° N), from November to July in the CT sector (18-20° N), and from October to July in the CB sector (20-22° N). Cold waters observed south of 12° N are not ascribable to upwelling events, but they are transported southwards by surface currents from the adjacent (northern) regions, as described in more detail in Subsection 3.3.

Time series of the monthly data, obtained from different sources (upwelling index, satellite data, wind products) and spatially averaged in the five sectors defined in the previous paragraph (Fig. 1b), were compared in order to describe the annual and inter-annual upwelling variability along the NW African coast (Subsections 3.1 and 3.2, respectively).

The horizontal patterns associated with the upwelling seasons were investigated by means of SST anomaly maps and drifter tracks in Subsection 3.3.

3.1. Annual evolution of the coastal upwelling conditions

The annual evolution of the UI_E, SST, and Chl-a, calculated by averaging the monthly data from 2009 to 2013, allows the illustration of the favorable upwelling conditions in the five sectors in Fig. 1b. The effect of the wind forcing (Ekman transport) on the ocean water is described in terms of presence of upwelled water (SST) and implications of upwelling for the ecosystem (Chl-a). Surface wind flux and coastal SST are two complementary parameters to quantify the spatial extent and intensity of the upwelling processes, the first one from physical theory and the second one based on direct observations (Benazzouz *et al.*, 2014).

The annual time series of UI_E are composed exclusively of positive values (Fig. 3a), and therefore downwelling conditions can be excluded in the entire study area. The Ekman transport shows conditions favourable to upwelling (> 150 m^3/s/100 m coastline) from January to June in the southern sectors (defined hereafter as SCV, CV), between January and July in the MA sector, and from February to December in the northern sectors (defined hereafter as CT and CB); it achieves its largest values in April, May, and June, respectively.

The annual cycle of SST (Fig. 3b) roughly follows the seasonal fluctuation outlined by UI_E (Fig. 3a). The SST increases gradually from north (CB sector) to south (SCV sector). According to the results of Fig. 2, an approximate threshold between the upwelling favourable/unfavourable conditions is defined at 24° C (Fig. 3b). The main differences with UI_E are observed during November, December, and January in the northern sectors, where the presence of cold upwelled waters is not supported by increments of the Ekman offshore transport (compare Figs. 3a and 3b).

In the southern and MA sectors, the Chl-a (Fig. 3c) increases gradually between October and May and drops in late spring, following the annual evolution of UI_E and SST. More precisely, Chl-a decreases in May in the SCV sector, in June in the CV sector, and in July in the MA sector, exhibiting a northward propagation in agreement with Lathuilière *et al*. (2008). Highest mean values, as large as 1.2 mg/m^3, are observed south of Cape Vert in April (SCV sector in Fig. 3c); lowest mean values (lower than 0.2 mg/m^3) are detected in June, July, and October in the MA sector. In the northern sectors, the Chl-a (Fig. 3d) shows an opposite behaviour: the Chl-a
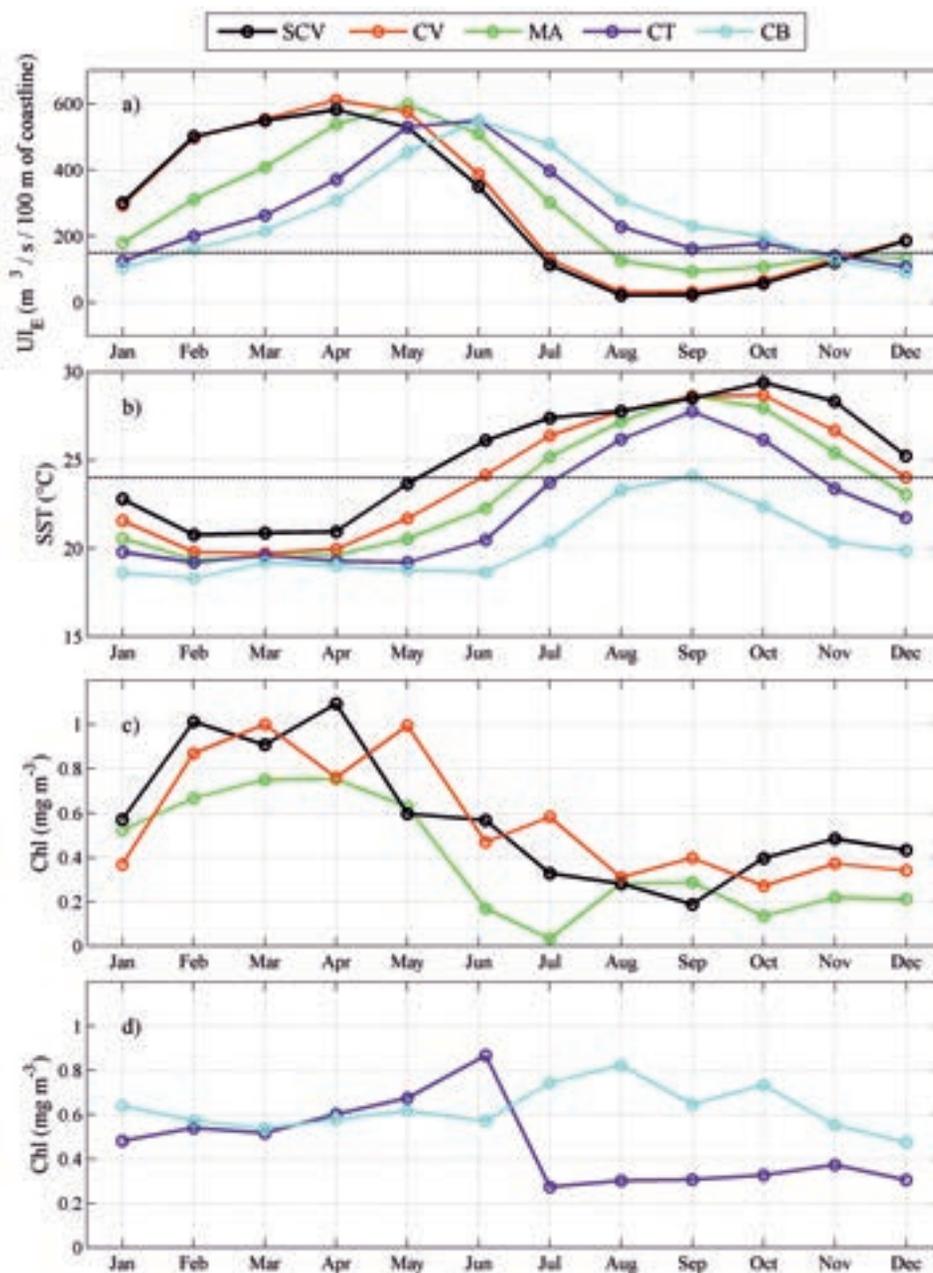
Fig. 3 - Annual cycle of the upwelling index UI_E, calculated from Ekman transport (a), SST (b), and Chl-a concentration (c, d), spatially averaged over the sectors depicted in Fig. 1b, during the period 2009-2013.

gradually increases/decreases between January and June in the CT/CB sectors, respectively; in July it drops in the CT sector and rises in the CB sector.

3.2. Inter-annual variability of the upwelling conditions

Time series of the monthly spatially averaged UI_E (Fig. 4a) and SST (Fig. 4b) summarize the main inter-annual characteristics of the upwelling seasons in the period 2009-2013. The Ekman
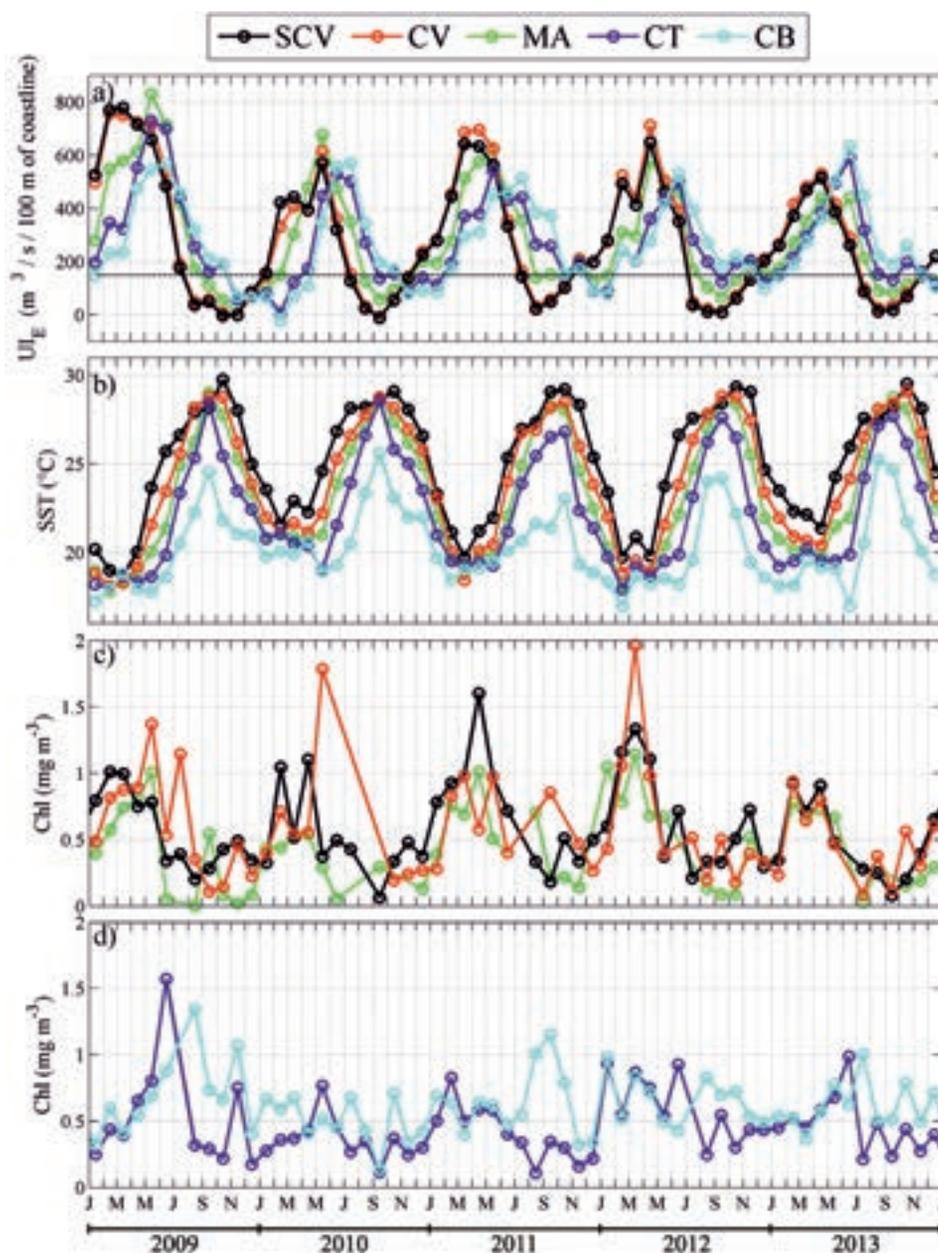
Fig. 4 - Inter-annual cycle of the upwelling index UI_E, calculated from Ekman transport (a), SST (b), and Chl-a concentration (c, d), spatially averaged over the sectors depicted in Fig. 1b, during the period 2009-2013.

transport is stronger in 2009 in comparison with the following years (Fig. 4a) and leads to SST colder than 18° C in the southern sectors (Figs. 2 and 4b). The fluctuations of UI_E (Fig. 4a) shows a phase shift between the southern sectors, where the maximum Ekman transport occurs between March and May, and the northern sectors, where the maximum occurs in June-July. The upwelling-favourable Ekman transport is generally larger in the southern and MA sectors, where it is in phase with the occurrence of the SST minimal values (Fig. 4b); indeed, the negative correlation between these two variables is largest at zero time lag (the correlation coefficient is

-0.89 in the southern sectors and -0.66 in the MA sector). The northern sectors display a time lag between the atmospheric forcing and the ocean response, with the largest negative correlation (~ -0.6) corresponding with a lag of 7-9 months.

The southern and MA sectors show the typical increase of the Chl-a during the months of upwelling (values generally larger than 0.5 mg/m^3 between February and May), and more accentuated increases in the SVC sector during the upwelling seasons 2011 (Fig. 4c) and in the CV sector during 2010 and 2012. In the CB sector (Fig. 4d) higher values of Chl-a are observed in summer (August-September) and early fall (October-November). The CT sector has no clear trend, with maxima values in the fall during 2009-2010, in winter in 2011 and 2012, and in spring in 2013 (Fig. 4d). The higher Chl-a concentration in the southern sectors, compared to the northern region, was already observed in Lathuilière *et al.* (2008) over the period 2000-2004, and was ascribed to the nutrient richness of subsurface water in this area caused by a shallow nutricline. Sometimes, similar increments of the UI_E in different sectors do not correspond to similar responses of the ecosystem, e.g., a similar increment of offshore Ekman transport in the SCV and CV sectors in March-April 2011 (Fig. 4a) corresponds with the maximum Chl-a in the SCV time series, but not in the CV time series (Fig. 4c). The strengthening/weakening of the offshore Ekman transport is indeed not sufficient to explain the Chl-a increase/decrease but, as suggested in Lathuilière *et al.* (2008), another process involved is the pre-existent nutrient availability in the surface layer. During winter, the nitrate surface concentration is quite high, indicating that the limitation by nutrient is weak [see Fig. 3d of Lathuilière *et al.*, (2008) and Fig. 7 of Deme-Gningue (1998)]. Therefore, a new input of nutrients by an upwelling-favourable wind event could not trigger an immediate and robust response of the ecosystem, as in winter/spring 2011 in the CV sector.

3.3. Upwelling seasons during 2009-2013

In this subsection, the COCES/COCES II drifter tracks, superimposed with the normalised SST anomaly maps, are used to describe the main circulation features related with the transport of cold waters during the upwelling seasons. Each figure contains four panels composed of consecutive 8-day SST anomaly maps (Figs. 5 to 8), specifically selected to emphasize the flow of cold water offshore and alongshore, overlapped with concurrent drifter trajectories (white lines).

In winter 2010, the SST anomaly maps define the occurrence of cold water filaments generated along the coast in correspondence to the capes (Cape Vert, Cape Timiris and Cape Blanc) and off the southern Mauritania coast at 16° -19° N (Fig. 5); they extend offshore for ~100-150 km with a mean temperature of ~18-20° C. Drifters deployed in the Cape Vert filament (Fig. 5a) record speeds of 30-40 cm/s and are mainly transported SW-wards (Figs. 5b and 5c). Cold water, originated from upwelling events south of Cape Vert, is transported southwards by surface currents, producing a tongue of cold water on the Gambia continental shelf (Figs. 5a and 5b). Drifters deployed in this region are transported southwards (Figs. 5a, 5b, and 5c) at a speed of 20-30 cm/s.

In spring 2011, two drifters deployed north of Cape Vert moved northwards parallel to the coast (Figs. 6a and 6b) at speeds greater than 40 cm/s, following the pathway of the MC, then turning westwards, transported by the filament of cold water located at ~18° N (Figs. 6c and 6d; speeds of 20-30 cm/s). The third drifter deployed north of Cape Vert was transported SW-wards
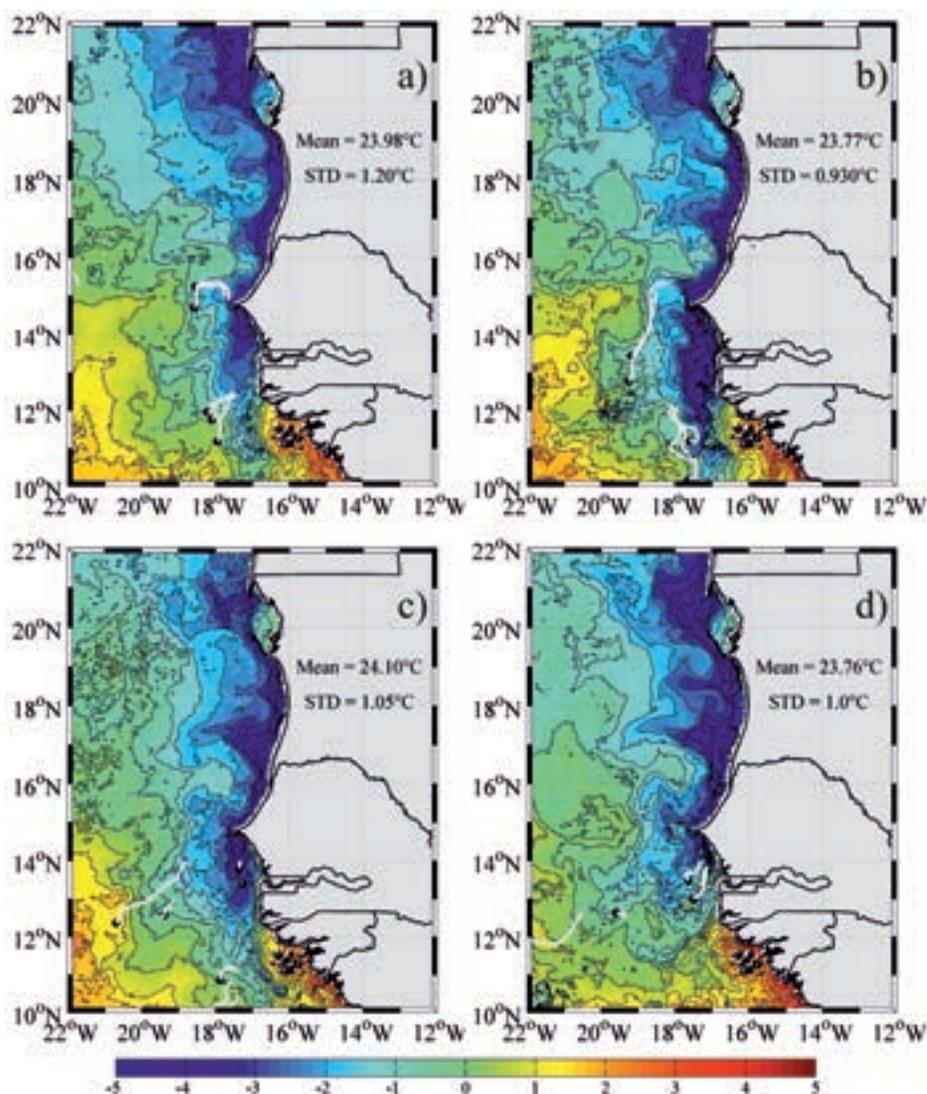
Fig. 5 - Normalised SST anomaly maps, derived from MODIS 8-day composite maps of SST, selected during the upwelling season 2010 with surface drifter tracks superimposed (white lines). MODIS maps are centred on February 17, 2010 (a), February 25, 2010 (b), March 5, 2010 (c), March 13, 2010 (d). Drifter ending points are shown with black circles. Mean values of SST and the relative standard deviation are reported in each panel.

(Figs. 6b, 6c, and 6d) at speeds greater than 30 cm/s. Cold water upwelling filaments are well defined in the second half of April (Figs. 6c and 6d), especially the Mauritania filament that extends offshore for more than 200 km. The cold water south of Cape Vert is mostly advected southwards; its southernmost extension occurs in late spring (Fig. 6d).

In winter-spring 2012, drifters deployed off Cape Vert moved northwards along the coast with speeds of 30 cm/s; (Figs. 7a and 7b) and turned westwards, following the upwelling filaments off the Mauritania coast (between 16.5° N and 18° N; Figs. 7b and 7d), or southwards (Fig. 7d), or were captured by mesoscale features (diameters of ~50 km) off the Senegal and Mauritania coasts (Figs. 7c and 7d). Drifters deployed south of Cape Vert (Fig. 7a) recirculated in the region of deployment (Figs. 7b and 7c), then were transported southwards (Fig. 7d).
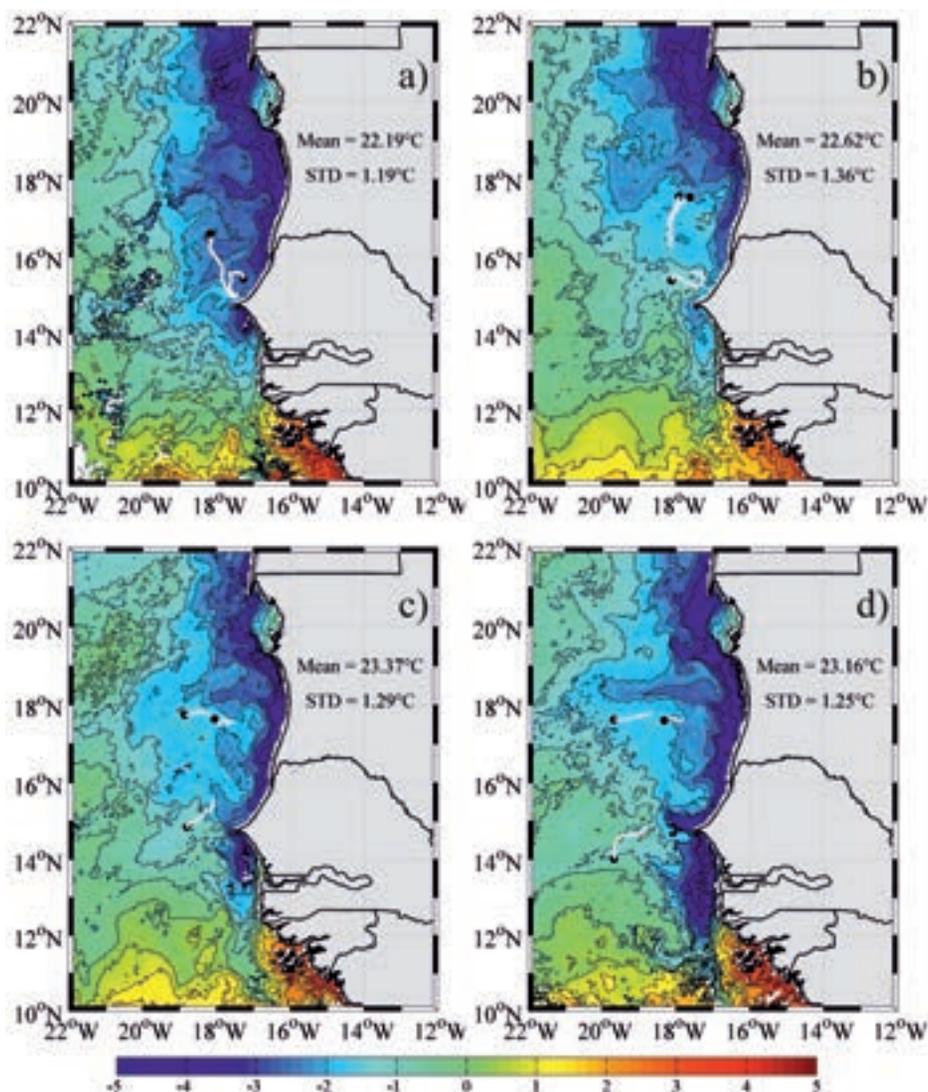
Fig. 6 - Normalised SST anomaly maps, derived from MODIS 8-day composite maps of SST, selected during the upwelling season 2011 with surface drifter tracks superimposed (white lines). MODIS maps are centred on April 6, 2011 (a), April 14, 2011 (b), April 22, 2011 (c), April 30, 2011 (d). Drifter ending points are shown with black circles. Mean values of SST and the relative standard deviation are reported in each panel.

In winter-spring 2013, a drifter deployed on the Senegal continental shelf south of Cape Vert moved northwards at speeds of 30-40 cm/s, showing the pathway of MC (Figs. 8a and 8b). Between 16° N and 17° N, drifters turned westwards (Fig. 8c) and were transported SW-wards (Fig. 8d) at speeds of 20-30 cm/s.

In summary, drifter tracks show the main meridional currents along the coast and zonal currents offshore. North of Cape Vert, the coastal circulation (<100 km from the coast) is directed polewards, whereas the main offshore westward currents are located in the region of the Mauritania filament (between 16.5° N and 18° N). South of Cape Vert, the coastal currents are directed toward the equator, and the offshore circulation is oriented SW-wards.
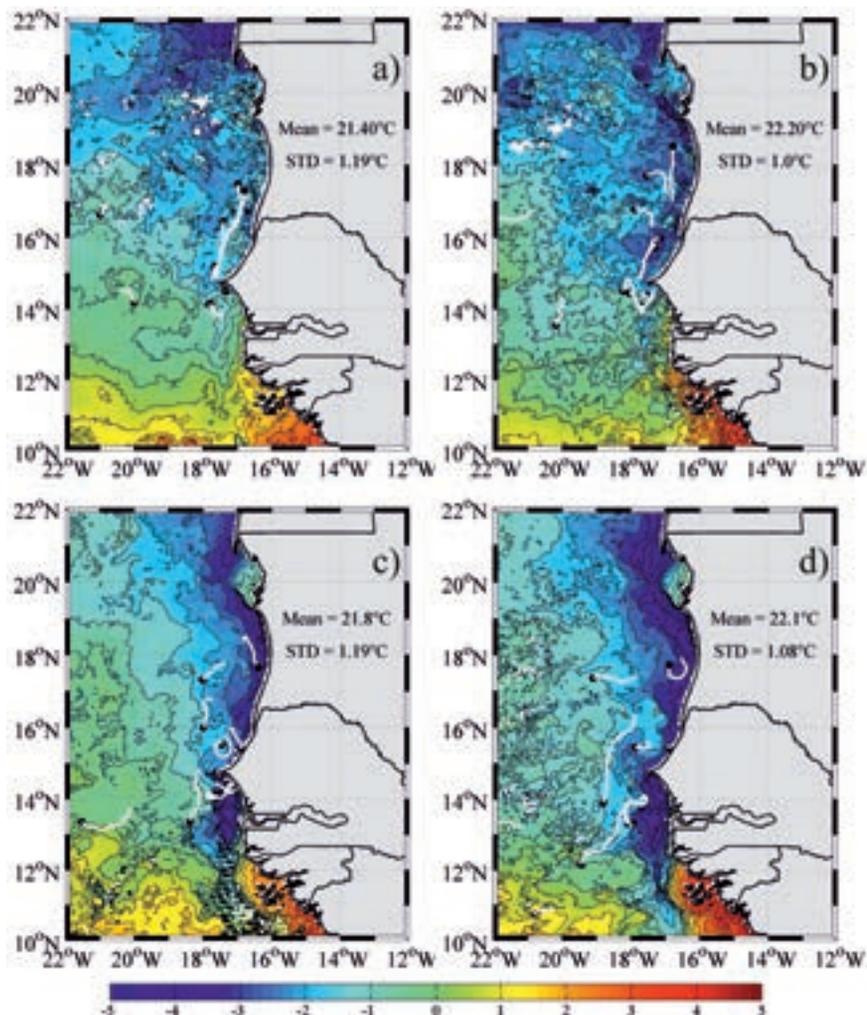
Fig. 7 - Normalised SST anomaly maps, derived from MODIS 8-day composite maps of SST, selected during the upwelling season 2012 with surface drifter tracks superimposed (white lines). MODIS maps are centred on March 12, 2012 (a), March 20, 2012 (b), March 28, 2012 (c), April 5, 2012 (d). Drifter ending points are shown with black circles. Mean values of SST and the relative standard deviation are reported in each panel.

4. Summary and discussion

Over the last few years, several works were carried out in order to describe and quantify the upwelling events in the CCUS. Nevertheless, most of these studies were mainly focused on the northern (Alvarez *et al.*, 2011) or southern areas (Ndoye e*t al.*, 2014) of the CCUS, and generally they considered the Senegal and Mauritania region as a unique system characterised by high seasonality (Benazzouz *et al.*, 2014) and modulated by the seasonal translation of the trade winds along the western African coast (Demarcq and Faure, 2000). This study proposes a deepened analysis of the Senegal and Mauritania coastal area in the period 2009-2013 and a comparative investigation of the different geographical sectors that compose this region. Upwelling conditions were analysed in terms of Ekman transport upwelling index and time series of the satellite SST, Chl-a, and wind products. The horizontal structure of the upwelling
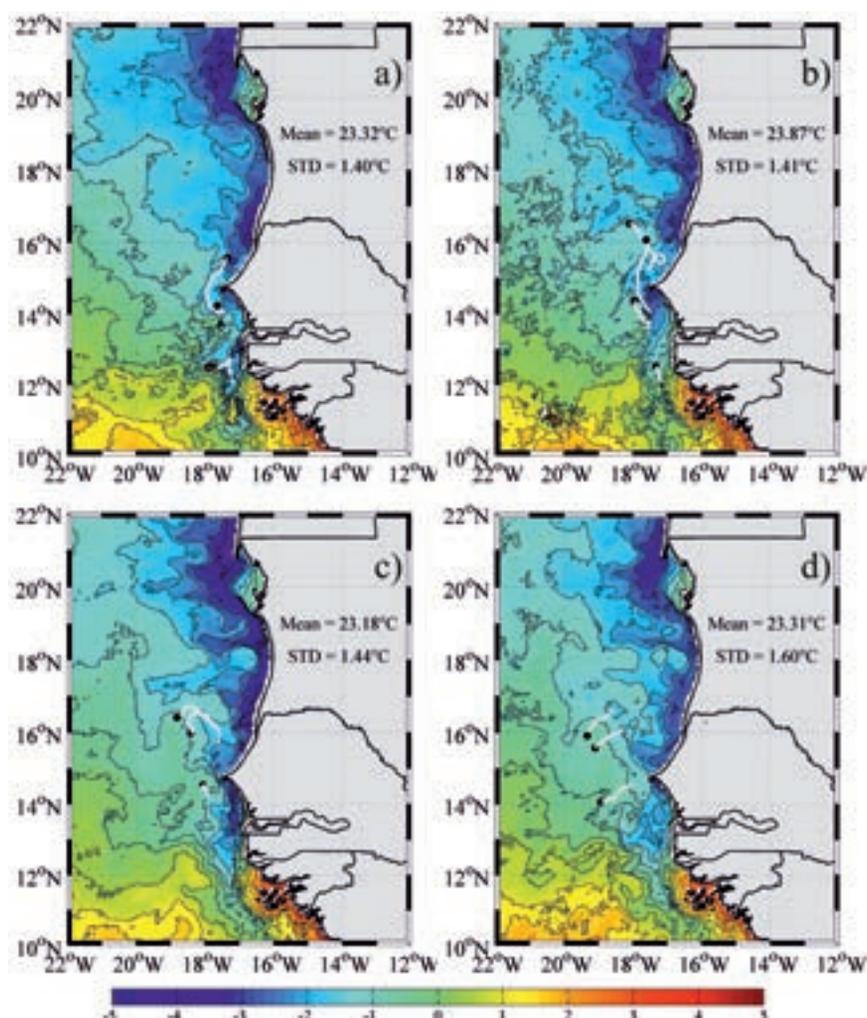
Fig. 8 - Normalised SST anomaly maps, derived from MODIS 8-day composite maps of SST, selected during the upwelling season 2013 with surface drifter tracks superimposed (white lines). MODIS maps are centred on March 13, 2013 (a), March 21, 2013 (b), March 29, 2013 (c), April 6, 2013 (d). Drifter ending points are shown with black circles. Mean values of SST and the relative standard deviation are reported in each panel.

processes was described using maps of SST anomalies and drifter tracks.

The area affected by upwelling is located north of 12° N, and the length of the upwelling seasons increases from south to north (Fig. 2). The mean annual evolution of UI_E (Fig. 3a) shows that the periods characterized by conditions more favourable to upwelling correspond to December-June in the southern sectors (SCV, CV) and to February-October in the northern sectors (CT and CB), with higher values (as large as 600 m^3 s^{-1}/100 m of coastline) in April/May and June, respectively. The fluctuation of wind forcing has a direct effect on the ocean water and on the ecosystem in the southern and in the MA sectors (Figs. 3b, 3c, and 3d), whereas the northern sectors are characterized by cold upwelled water even in the months with low values of UI_E.

In the southern sectors, the inter-annual evolution UI_E and SST are in phase (higher values of UI_E correspond with lower SST; Figs. 4a and 4b), which means that the upwelling is tightly linked to the seasonality of the trade winds, without time lag, in agreement with the results of

Benazzouz *et al*. (2014) in the same area. The northern sectors show a fluctuation that is out of phase with respect to the southern sectors (Fig. 4a), with a lag between the atmospheric forcing and the ocean response of about 7-9 months. Cropper *et al*. (2014) have observed an increase of the summer downwelling favourable conditions south of 19° N in the period 1981-2012; this trend is confirmed by the results of the present study, which show a weakening of the Ekman offshore transport during 2009-2013.

The implications of the upwelling for the ecosystem have been characterised using the time series of the Chl-a concentrations (Figs. 4c and 4d). In the southern sectors, Chl-a shows a high variability related to the occurrence of upwelling and non-upwelling seasons; the highest concentration values are observed in the SCV sector during the upwelling seasons of 2011 and in the CV sector during 2010 and 2012 (Fig. 4c). In the northern sectors, the Chl-a shows a high inter-annual variability not affected by the seasonal upwelling fluctuation (Fig. 4d). The two distinct behaviours of the Chl-a along the Senegal and Mauritania coasts were already detected by Lathulière *et al*. (2008). These authors have distinguished the region between 10° N and 19° N, characterised by a large seasonal cycle and by a significant correlation with the wind stress, from the region between 19° N and 24° N, characterised by a small amplitude of the seasonal cycle and no significant correlation with the wind stress.

The maps of SST anomalies allow the discrimination of the cold water filaments associated with the upwelling events along the Senegal and Mauritania coast. These recurrent upwelling filaments (SST lower than 18° C) are generally located north of Cape Vert, off the southern Mauritania coast, south of Cape Timiris, and in the Cape Blanc area (Figs. 5 to 8). The filaments persist for a few weeks, and they subsequently mix with the surrounding waters. The filament formation off the capes is generally associated with the topographic and coastline morphology of the region. This dynamical process is common to the other upwelling regions as explained by Dale and Barth (2001), with important implications for the transport of shelf water to the deep ocean (Barth *et al*., 2000). The wind vorticity reinforces the upwelling near the capes via Ekman pumping, as seen along the California coast (Paduan and Niiler, 1990) or in the Adriatic (Poulain *et al*., 2004b). Tongues of cold water can be observed on the Senegal continental shelf south of Cape Vert in the region between 10° N and 15° N; the southernmost extension of these tongues occurs in spring in corroboration with Roy (1998), Demarcq (1998) and Demarcq and Faure (2000).

Drifter tracks allow the addition of details about the flow of cold water offshore and alongshore. In particular, they describe: 1) the westward zonal transport of waters from the coast toward the Cape Vert Archipelago in correspondence with the Mauritania coast (Figs. 6c, 6d, 7d, 8d); 2) the SW-ward transport of the coastal water in the region of Cape Vert and south of Cape Vert (Figs. 5, 7c, 7d); 3) the northward MC off the Senegal and Mauritania coasts (Figs. 6a, 7a, 7b).

5. Conclusions

This work contributes to and improves the knowledge about the variability of the Senegal and Mauritania upwelling system over seasonal and interseasonal timescales. Previous works have already emphasized strong latitudinal variations along the coast, in particular between the northern and the southern ends of CCUS, but the geographical limits of the sectors with similar

characteristics were not precisely defined and the Senegal and Mauritania coasts were frequently classified as a unique system with homogeneous features. The results of this work show a gradual increase of the length of the upwelling season with the latitude and lead to the definition of two regions along the Senegal and Mauritania coasts with fairly different behaviour: a northern sector that includes the region off Cape Blanc and Cape Timiris (north of 18° N) and a southern sector, located south of 16° N.

In the northern sector, the cold upwelled waters are detected between October and July, and their presence does not appear influenced by the annual fluctuation of Ekman transport, which shows upwelling-favourable conditions between February and October. The maximum annual value of the Chl-a is 0.8-0.9 mg/m^3. The southern sector exhibits strong seasonal variations, and the core of the upwelling season occurs from December to June. The fluctuation of wind forcing plays a direct effect on the ocean water and on the ecosystem response, without time lag. The Chl-a increases gradually from October to May and drops in late spring.

The main limitation of this approach is that 5-year time series are too short to clearly define a trend in the upwelling and to correlate the inter-annual variation of the variables with large-scale and local climatic patterns. This issue can constitute a starting point for a future analysis, which would take into account longer time series of satellite and in-situ data and their relation with global atmospheric teleconnection patterns.

REFERENCES

Alpers W., Brandt P., Lazar A., Dagorne, D., Sow B., Faye S., Hansen M.W., Rubino, A. Poulain, P.-M. and Brehmer, P.; 2013: *A small-scale oceanic eddy off the coast of West Africa studied by multi-sensor satellite and surface drifter data.* Remote Sens. Environ., **129**, 132-143.

Alvarez I., Gomez-Gesteira M., de Castro M., Lorenza M.N., Crespo A.J.C. and Dias J.M.; 2011: *Comparative analysis of uwelling influence between the western and northern coast of the Iberia Peninsula.* Cont. Shelf Res., **31**, 388-399.

Aristegui J., Alvarez-Salgado X.A., Barton E.D., Figueiras F.G., Hernandez-Leon S., Roy, C. and Santos A.M.P.; 2004: *Oceanography and fisheries of the Canary Current/Iberia region of the eastern North Atlantic.* The Sea, **14**, 877-931.

Aristegui J., Barton E.D., Alvarez-Salgado X.A., Santos M., Figueiras F.G., Kifani S., Hernandez-Leon S., Mason E. and Demarcq H.; 2009: *Sub-regional ecosystem variability in the Canary Current upwelling.* Prog. Oceanogr., **83**, 33-48.

Barth J.A., Pierce S.D. and Smith R.L.; 2000: *A separating coastal upwelling jet at Cape Blanco, Oregon, and its connection to the California Current system.* Deep-Sea Res. Pt. II, **47**, 783-810.

Barton E.D.; 1998: *Eastern boundary of the North Atlantic: Northwest Africa and Iberia.* In: Robinson A.R. and Brink K.H. (eds), The sea, the global coastal ocean: regional studies and syntheses, New York, Vol. 11, pp. 633-657.

Benazzouz A., Mordane S., Orbi A., Chagdali M., Hilmi K., Atillah A., Pelegrí, J.L. and Demarcq H.; 2014: *An improved coastal upwelling index from sea surface temperature using satellite-based approach – The case of the Canary Current upwelling system.* Cont. Shelf Res., **81**, 38-54.

Copper E.T., Hanna E. and Bigg G.R.; 2014: *Spatial and temporal seasonal trends in coastal upwelling off Northwest Africa, 1981-2012.* Deep Sea Res., **86**, 94-111.

Dale A.C. and Barth J.A.; 2001: *The hydraulics of an evolving upwelling jet flowing around a cape.* J. Phys. Oceanogr., **31**, 226-243.

Davis R.E.; 1985: *Drifter observations of coastal currents during CODE. The method and descriptive view.* J. Geophys. Res., **90**, 4741-4755.

Demarcq H.; 1998: *Spatial and temporal dynamics of the upwelling off Senegal and Mauritania: local change and trend*. In: Durand M.H., Cury P., Mendelssohn R., Roy C., Bakun A. and Pauly D. (eds), Global versus local changes in upwelling systems, ORTSOM ed., Paris, pp. 149-166.

Demarcq H. and Faure V.; 2000: *Coastal upwelling and associated retention indices derived from satellite SST. Application to Octopus vulgaris recruitment*. Oceanol. Acta, **23**, 391-408.

Deme-Gningue I.; 1998: *Trends and variability of environmental time series along the Denegalese coast*. In: Durand M.H., Cury P., Mendelssohn R., Roy C., Bakun A. and Pauly D. (eds), Global versus local changes in upwelling systems, ORSTOM ed., Paris, pp. 179-192.

Doi T., Tozuka T. and Yamagata T.; 2009: *Interannual variability of the Guinea Dome and its possible link with the Atlantic Meridional Mode*. Clim. Dyn., **33**, 985-998, doi: 10.1007/s00382-009-0574-z.

Gomez-Gesteira M., de Castro M., Alvarez I., Gomez-Gesteira J.L.; 2008: *Coastal sea surface temperature warming trend along the continental part of the Atlantic Arc (1985–2005)*. J. Geophys. Res., **113**, C04010, doi:10.1029/2007JC004315.

Hansen D.V. and Poulain P.-M.; 1996: *Processing of WOCE/TOGA drifter data*. J. Atmos. Ocean. Tech., **13**, 900-909.

Lathuiliére C., Echevin V. and Lévy M.; 2008: *Seasonal and interseasonal surface chlorophyll-a variability along the northwest African coast*. J. Geophys. Res., **113**, C05007, doi: 10.1029/2007JC004433.

Lázaro C., Fernandes M.J., Santos A.M.P. and Oliveira P.; 2005: *Seasonal and interannual variability of surface circulation in the Cape Verde region from 8 years of merged T/P and ERS-2 altimeter data*. Remote Sens. Environ., **98**, 45-62.

Lumpkin R. and Garzoli S.L.; 2005. *Near-surface circulation in the Tropical Atlantic Ocean*. Deep-Sea Res. I, **52**, 495-518.

Mason E., Colas F., Molemaker J., Shchepetkin F., Troupin C., McWilliams J.C. and Sangrà P.; 2011: *Seasonal variability of the Canary Current: A numerical study*. J. Geophys. Res., **116**, C06001.

Marchesiello P., Herbette S., Nykjaer L. and Roy C.; 2004: *Eddy-driven dispersion processes in the Canary Current upwelling system: comparison with California System*. GLOBEC International newsletter, **10**(1).

Meunier T., Barton E.D., Barreiro B. and Torres R.; 2012: *Upwellng filaments off Cap Blanc: interaction of the NW African upwelling current and Cape Verde frontal zone eddy field?* J. Geophys. Res., **117**, C08031, doi: 10.1029/2012JC007905.

Mittelstaedt E.; 1991: *The ocean boundary along the northwest African coast: circulation and oceanography properties at the sea surface*. Prog. Oceanogr., **26**. 307-355.

Ndoye S., Capet X., Estrade P., Sow B., Dagorne D. and Lazar, A.; 2014: *SST patterns and dynamics of the Southern Senegal-Gambia upwelling center*. J. Geophys. Res. Oceans, **119**, 8315-8335.

Paduan J.D. and Niiler P.P.; 1990: *A Lagrangian description of motion in Northern California coastal transition filaments*. J. Geophys. Res., **95**, C10, 18095-18109, doi: 10.1029/JC095iC10p18095.

Poulain P.-M., Barbanti R., Cecco R., Fayes C., Mauri E., Ursella L. and Zanasca P.; 2004a: *Mediterranean surface drifter database: 2 June 1986 to 11 November 1999*. Rel. 75/2004/OGA/31, OGS, Trieste, Italy, CD-Rom.

Poulain, P.-M., Mauri, E. and Ursella L.; 2004b: *Unusual upwelling event and current reversal off the Italian Adriatic coast in summer 2003*. Geophys. Res. Lett., **31**, L05303, doi: 10.1029/2003GL019121.

Roy C.; 1998: *An upwelling-induced retention area off Senegal: a mechanism to link upwelling and retention processes*. S. Afr. J. Marine Sci., **19**, 89-98.

Santos A.M.P., Kazmin A.S. and Peliz A.; 2005: *Decadal changes in the Canary upwelling system as revealed by satellite observations: their impact on productivity*. J. Marine Res., **63**, 359-379.

Stramma L., Huttl S. and Schafstall J.; 2005: *Water masses and currents in the upper tropical northeast Atlantic off northwest Africa*. J. Geopys. Res., **110**, C12006. doi: 10.1029/2005JC002939.

Sybrandy A.L. and Niiler P.P.; 1991: *WOCE/TOGA Lagrangian drifter construction manual*. SIO Ref. 91/6, WOCE REP. 63, Scripps Institution of Oceanography, La Jolla, California, 58 pp.

Wooster W.S., Bakun A. and Mclain D.R.; 1976: *Seasonal upwelling cycle along Eastern boundary of North-Atlantic*. J. Mar. Res., **34**, 131-141.

Corresponding author: Milena Menna
OGS, Borgo Grotta Gigante, 42/c, 34010 Sgonico (TS), Italy
Phone: +39 3383019108; fax: +39 040327307; e-mail: mmenna@ogs.trieste.it